Environment Friendly Binderless Cellulose Based Thermal Insulation Building Material Made of Forestry Waste

Zoltán Pásztory[1*], *Diogo* Machado Neto[2], *Alexandre* Ottolini[2], *Zsófia* Kóczán[1], *Tibor* Horváth[4], *Bao* Ngoc Nguyen[5], and *Mihály* Bariska[3]

[1] University of Sopron, Faculty of Wood Engineering and Creative Industries, 4. Bajcsy-Zs. str. Sopron 9400, Hungary
[2] Cesi, Campus de Angouléme, La Couronne, 40 rte. Croic do Milieu, Angouléme, France
[3] Formerly at ETH, Zürich, Höngeberg, Switzerland
[4] Woodspring Ltd., 108 Gerinc str. Budapest 1221, Hungary
[5] Research Institute of Forest Industry – Vietnamese Academy of Forest Sciences, 46 Duc Thang – Bac Tu Liem – Ha Noi, Vietnam

Abstract. This research investigates environmentally friendly, binderless thermal insulation fibreboards utilizing three types of raw materials. The primary objective was to evaluate the usability of forest residues. For comparison, the same production process was applied to sawdust residues from hybrid poplar (*Populus euramericana*) and Scots pine (*Pinus sylvestris*). Five processing variations were applied to the undergrowth biomass, including treatment with a Hollander beater for 20, 40, and 60 minutes to optimize the final product properties. The samples were characterized based on density, equilibrium moisture content, morphology, porosity, thermal stability, and thermal conductivity. Among the tested approaches, the samples produced from forest residue with 40 minutes of Hollander beater treatment achieved the most favorable balance of properties. The best thermal conductivity was 0.0691 W/m·K, moderate density, and improved porosity (53.38%), closely matching the performance of the poplar-based panels. Conversely, pre-soaking biomass in water for three days increased density and moisture content, negatively impacting thermal performance. Thermogravimetric analysis confirmed that the thermal stability of the forest residue panels was comparable to those made from traditional pine and poplar sawdust. FTIR analysis indicated that the self-bonding properties were primarily facilitated by the inherent lignin and hemicellulose content of the raw materials.

1 Introduction

In Europe, the building sector accounts for approximately 40% of final energy consumption. This significant share is one of the main reasons behind the goal of achieving a carbon-neutral building sector by 2050. Over recent decades, the operational energy use of both residential

* Corresponding author: pasztory.zoltan@uni-sopron.hu

and non-residential buildings has been responsible for 26% of CO_2 emissions — 8% of which are direct emissions, and 18% indirect, stemming from electricity and heat production. To meet the "Net Zero Emissions by 2050" scenario Buildings - Energy System – IEA, it is crucial to accelerate the transition toward more sustainable practices.

In response, a global trend is emerging that urges construction companies to reassess their carbon footprint. One increasingly popular solution is the use of bio-based materials, which are renewable and easier to produce compared to mineral-based alternatives. Currently, the construction sector consumes around 50% of all extracted materials, leading to substantial CO_2 emissions. A complete shift to wood-based construction could significantly reduce these emissions. However, this would create an annual demand of 400 million cubic meters of wood — equivalent to roughly 50% of Europe's annual forest growth. A study forecasting the scale of wood residues in Europe by 2025 estimates that Finland, with 70% of its land covered by forest, could generate between 14 and 16 million tonnes of such residues [1].

This approach aligns with European Directive 2008/98/EC, which prioritizes waste prevention, followed by reuse and recycling. Energy recovery and landfilling are considered last options. For instance, in France, 4.2 million tonnes of green waste were collected at waste collection centres in 2017. Wood fibre panels used for thermal insulation typically have a density range between 50–270 kg/m³ [2]. Based on these values, France alone could produce between 15,555 and 84,000 m³ of insulation material from the collected green waste.

Fibreboard has been produced for many years, traditionally using synthetic binders — most commonly formaldehyde-based resins. These binders have come under increasing scrutiny, as formaldehyde is classified as a Category 1B carcinogen by the International Agency for Research on Cancer. In addition, materials manufactured with synthetic binders are difficult to recycle and pose environmental concerns. Recently, research has shifted towards binderless fibreboard production, which is less harmful to the environment during manufacturing and allows for easy recycling. At the same time, the reuse of industrial and construction by-products has become increasingly popular. However, this popularity has led to increased demand for and rising prices of these materials.

Wood chips, for example – representing approximately 7.5% of a tree after processing – saw a price increase of 30% between 2006 and 2011. To keep wood fibre insulation materials competitive in the construction market, reducing production costs is essential. Van Dam et al. [3] reported that the cost structure of these products is roughly composed of 34% binder, 32% wood, 24% labour, and 10% energy. To develop eco-friendly and cost-effective fibreboard, it is therefore valuable to explore alternative raw materials that are more affordable than wood chips and suitable for binder-free production. This approach could represent a significant step forward in the field of eco-construction. One of the main novelties of this research that uses a very low value undergrowth biomass materials with a low quality to producing high value building materials can be replace synthetic materials.

The primary objective of a recent study was to expand the range of raw materials for fibre-based insulation by using forest residues mixed with undergrowth collected during forest maintenance operations which is handled waste today. A secondary objective was to eliminate adhesives entirely and investigate the self-bonding potential of cellulose-based materials. The goal was to create an environmentally friendly insulation material that can be easily recycled. The performance of these new panels was then compared to panels made from pine and poplar residues.

2 Materials and methods

Three types of raw materials were used for the laboratory production of environment friendly binderless thermal insulation materials. The primary objective of the research was to evaluate the usability of forest residues left on-site after tree harvesting and area maintenance. This

biomass primarily consists of small tree branches with a high bark content, chipped wood pieces, and, to a lesser extent, weeds and bush residues. Originally these materials are leaved on the site to be rotten. Forest residues were collected and coarsely chipped from the botanical garden of the University of Sopron (Sopron, Hungary).

For comparison, the same production process was applied to poplar and pine chips obtained from the sawmill of KEFAG Zrt., located in central Hungary. These materials were residues from sawing hybrid poplar (*Populus euramericana*), commonly known as Pannonia poplar and pine (*Pinus sylvestris*). The poplar and pine sawdust was produced by bandsaw and were handled as wood waste, and used to burn them for producing energy. The moisture content of the sawdust was slightly below the fiber saturation point. The particle sizes of both pine and poplar sawdust were suitable for the production method used.

The raw materials obtained from routine maintenance of the botanical garden park were first shredded into chips. These materials were then stored in aerated boxes in the laboratory. Five processing variations were applied to each raw material type to investigate the effects of different manufacturing methods on the final properties of the fibreboards (Table 1). For each fibreboard type, 3 kg of raw material was used. Defibration was performed using a wet process in four steps, employing different gap sizes between the disc type refinery machine's plates to effectively separate all fibres comprising the raw material.

Samples B0, B1, B2, B3, and B4 were produced from undergrowth biomass, each with specific processing variations to assess their impact on the results. In addition to defibration, B1, B2, and B3 were treated using a Hollander beater for 20, 30, and 40 minutes, respectively. With B4, the impact of water before defibration on the raw materials and on the properties of the resulting material was analysed. Pine, poplar, and B0 were produced in the same way with disc refinery and no Hollander beater were used.

After these initial steps, the samples were placed into moulds to form the desired shape and allow excess water from the wet process to drain. This produced a wood fibre panel solid enough to be handled and placed in an oven at 80 °C for curing.

Table 1. Sample production.

Identification	Pretreatment	Defibration in wet process	Hollander beater	Moulded	Oven
Pine	no	Gap sizes: 1 mm / 0.6 mm / 0.3 mm / 0.1 mm	no	50 cm diameter	80°C
Poplar	no		no		
B0	no		no		
B1	no		20 min		
B2	no		40 min		
B3	no		60 min		
B4	3 days in water		no		

2.1 Density measurements

To measure the density, each sample was cut into cubes of 30 ± 1 mm and pre-conditioned at 65% RH and 20 °C. Prior to testing, the mass of each sample had to be constant. For each group, 15 specimens were measured using an electronic calliper in accordance with the standard EN 325.

2.2 Equilibrium moisture content in normal climate

We used pre-conditioned samples under the same conditions as for the density measurements, that is, 65% RH at 20 °C, and cut into 30 ± 1 mm cubes. The initial weight of five specimens from each group was recorded before placing them in an oven at 103 °C for drying. The weight was measured daily, and the drying process was considered complete once the variation in mass was less than 0.1%.

2.3 Morphology

The sizes of the wood fibres were analysed using a TAGARNO FHD microscope to assess the impact of pre-treatments on fibre length and width. A total of 150 fibres were measured for length and 75 for width using a 50x magnification lens (Fig. 1).

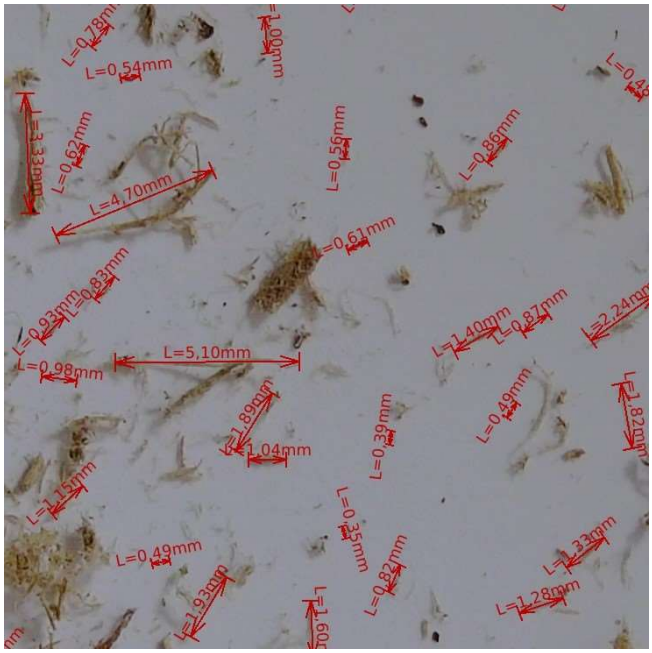

Fig. 1. Image for morphology measurements.

2.4 Porosity

To measure the porosity of the different materials, samples from each fibreboard are cut into sticks with a surface area of 1 cm². These samples are then embedded in epoxy resin with a low viscosity (Elan Tech EC 141 NF). After the curing process, three thin slices of 40 µm thickness are cut from each sample using a microtome. For each layer, five images are captured using a TAGARNO FHD Microscope equipped with a 50x lens and a 156x zoom. The images are then analysed using ImageJ software (Fig. 2).

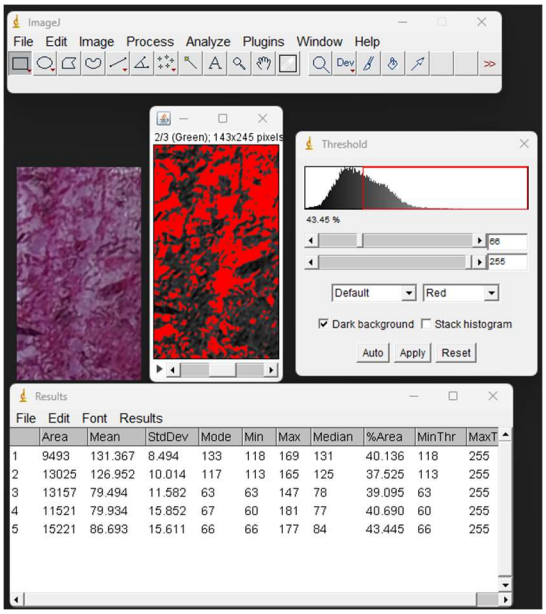

Fig. 2. ImageJ software used to determine the porosity area.

2.5 Spatial arrangement of fibres

The spatial arrangement of the fibres was analysed using a Scanning Electron Microscope (SEM), specifically the Hitachi S-3400N model from Japan. Imaging was conducted at various magnifications (×55, ×200 and ×300) and at an accelerating voltage of 20 kV. This analysis provided detailed insights into fibre morphology influenced by different mechanical treatments, the quality of internal bonding, and a visual assessment of porosity distribution and fibre orientation within the material.

2.6 Infrared spectrometry

To analyse the internal bonding within the material on a molecular scale, we use Fourier Transform Infrared Spectroscopy (FTIR), model FT/IR-6300, performing four measurements on each fibreboard.

2.7 Thermal conductivity

Thermal conductivity was measured using the hot plate method, with a standardized temperature range of 5 °C on the cold side and 15 °C on the hot side. To ensure one-dimensional heat flow, 15 cm thick insulation was placed around the sample. The heat flow occurred perpendicularly from the hot side to the cold side, allowing for the accurate determination of the sample's thermal conductivity (Fig. 3). The measurement began once the fluctuation of the last readings per minute was below 0.002 W/m·K, indicating a steady state [4]. To improve accuracy, 100 measurements were taken, and the final result was calculated as the average of these values. Each measurement took one minute, meaning the entire measurement process lasted 100 minutes.

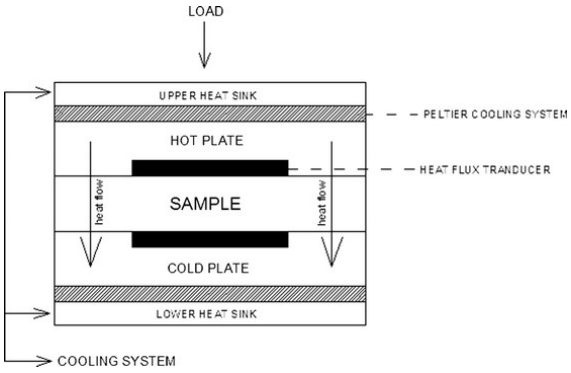

Fig. 3. Scheme of the heat flow measurement setup for the insulation fibreboards.

2.8 Thermogravimetry

Thermogravimetric analysis was conducted using a Setaram Labsys Evo 1150 °C (France) instrument. Nitrogen served as the carrier gas, with an airflow rate of 50 ml/min. The temperature range was set from 30 °C to 800 °C, with a heating rate of 10 °C/min. Corundum crucibles were used as sample holders, and approximately 25 mg of sample was placed in each crucible. Correction measurements were performed to account for buoyancy effects.

3 Results and discussions

3.1 Density

Table 2 shows the density results for each type of fibreboard (for sample´s labels see Table 1). The density of bush-based panels ranges from 184.74 kg/m³ to 204.57 kg/m³. It decreases by approximately 6 kg/m³ after 20 minutes of treatment with the Hollander beater, then increases by about 1.5 and 6.75 kg/m³ after 40 and 60 minutes of treatment, respectively.

Table 1. Density measurement.

Samples	**Density (kg/m³) average ± s.d.**	**Moisture content (%) average ± s.d.**
B0	184.74 ± 3.67	15.98 ± 0.40
B1	178.81 ± 8.27	15.61 ± 0.71
B2	180.27 ± 8.76	12.87 ± 0.59
B3	185.56 ± 4.69	13.35 ± 0.97
B4	204.57 ± 6.70	19.70 ± 0.70
Pine	179.24 ± 2.16	13.54 ± 1.15
Poplar	165.56 ± 5.05	12.22 ± 0.65

Notably, the density of B4 is nearly 20 kg/m³ higher than that of B0. This difference may be attributed to variations in moisture content and fibre size, as presented in Tables 2 and 3, respectively. Despite using the same process, the initial densities of B0, pine and poplar differ. This discrepancy can be explained by the inherent differences in the specific densities of the raw materials, as well as their responses to defibration, which affects porosity. When compared to wood fibreboards reported by Hung Anh and Pásztory [5], which have densities

ranging from 30 to 270 kg/m³, the samples in this study can be classified as medium- to high-density fibreboards.

3.2 Equilibrium moisture content in normal climate

Table 2 shows that the highest equilibrium moisture content was observed in B4. Soaking in water appears to increase the equilibrium moisture content of the material. The Hollander beater also seems to influence this equilibrium, as B1, B2, and B3 — treated for 20, 40, and 60 minutes, respectively — exhibited lower equilibrium moisture contents compared to B0, which was not treated. Furthermore, B2, despite having a higher density than poplar, reaches an equilibrium moisture content similar to that of poplar, likely due to the effects of its treatment.

Like density, moisture content influences the λ-value, and this impact varies with temperature. At lower temperature differences, moisture content tends to be relatively uniform, but at higher temperature differences, vapor diffusion within the material occurs, which also leads to the transfer of vapor enthalpy. After the thermal conductivity measurements, we observed condensation on the cold side of the material, which confirms this phenomenon. As moisture content increases, mechanical strength decreases, while thermal conductivity increases. Water is present in wood in two forms: through hygroscopic attraction and capillary action, both are influenced by the wettability and the density of the fibre substance.

3.3 Morphology

Table 3 presents the dimensions of the fibres (diameter and length), and it can be seen that the standard deviation is of the same order of magnitude as the average, indicating poor homogeneity in fibre sizes within the material. B0 and B4 were treated similarly, with the difference that B4 was submerged in water for three days before mechanical refining. Given the differences in fibre sizes between the two materials, it can be deduced that water treatment facilitated easier fibre detachment. The longer fibres of B4 suggest that they passed more quickly through the defibration discs. Table 2 also shows that B4 has the highest moisture content due to its pre-treatment. Both B0 and B4 show poor homogeneity.

Table 3. Dimensions of fibres at fibreboards.

Specimens	Length (mm) average ± s.d.	Width (mm) average ± s.d.
B0	1.35 ± 1.38	0.19 ± 0.13
B1	1.23 ± 0.89	0.16 ± 0.11
B2	1.37 ± 0.97	0.18 ± 0.12
B3	1.50 ± 1.23	0.23 ± 0.20
B4	1.64 ± 1.79	0.23 ± 0.29
Pine	1.36 ± 1.03	0.44 ± 0.23
Poplar	1.25 ± 0.74	0.24 ± 0.19

These results also allow the study of the influence of the Hollander beater on fibre sizes in B1, B2, and B3 fibreboards. For these three materials, it can be observed that longer treatment times lead to larger fibre dimensions but with decreasing homogeneity. Pine and

poplar exhibit some of the smallest fibre dimensions – except for the diameter of pine fibres – and they also demonstrate the best homogeneity rates.

The size of the fibres in fibreboard insulation materials is an important parameter because it influences porosity, density, moisture content, and mechanical properties. A broad and continuous particle size distribution improves the material's mechanical properties. Previous research [6] suggests that a uniform fibre size leads to more homogeneous porosity compared to other wood-based insulation materials, such as oriented strand board (OSB).

The greater width of the B4 fibres compared to B0 is probably due to the higher moisture content, as illustrated in Figure 4.

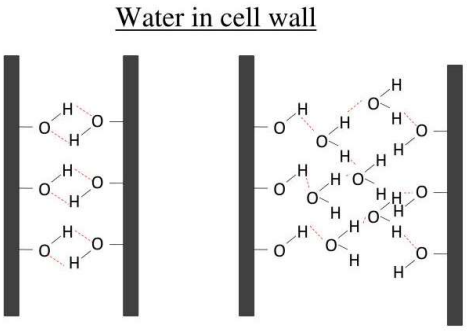

Fig. 4. Scheme of influence of hygroscopicity in hydrogen bonds according to [14].

3.4 Porosity

As shown in Table 4, the highest porosity is achieved by poplar, which also has the lowest density. It can also be observed that B1, B2, and B3 exhibit higher porosity rates than B0, indicating that treatment with the Hollander beater improves the material's porosity. Forty minutes of treatment appears to be optimal, as B2 shows 53.38% porosity, just behind poplar.

Table 4. Porosity rate of the different samples.

Specimens	**Porosity (%) average ± s.d.**
B0	40.18 ± 2.19
B1	48.05 ± 3.58
B2	53.38 ± 2.58
B3	45.23 ± 3.18
B4	40.74 ± 3.04
Pine	50.42 ± 4.27
Poplar	55.33 ± 5.43

In solid materials, porosity has various effects: it increases both thermal and acoustic insulation while decreasing the bulk density. According to Shrestha et al. [7], as porosity increases, sound velocity decreases linearly. A similar trend is observed in thermal insulation: the higher the porosity, the lower the thermal conductivity, since air has a lower λ-value than wood. The results obtained in this study are lower than those reported in the literature [8], which may explain the medium to high thermal conductivity of our fibreboards. This relatively low porosity is not due to the type of raw material, but rather to the manufacturing

process. The downward flow of excess water during production creates pressure on the material, leading to compression.

3.5 Scanning electron microscope (SEM)

SEM analysis provides insights into the arrangement of fibres within the material, as well as the effects of different treatments on fibre quality. As shown in Figure 5, the fibres appear disorganised and damaged due to the defibration process. SEM can also be used to examine the distribution of voids, and Figure 5 indicates that they are not uniformly distributed throughout the material matrix.

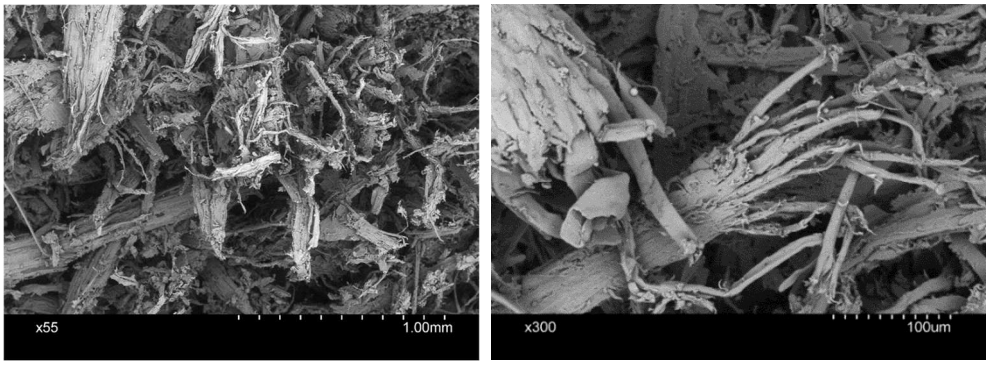

Fig. 5. SEM micrographs of B0 ×55 (left) ×300 (right).

After the different stages of disc refining, we obtain irregularly shaped fibres of varying sizes. This phenomenon is further intensified by the Hollander beater, as shown in Figure 6, leading to the formation of microscopic voids between the fibres. Figure 6 illustrates the varying impact of the Hollander beater on the fibres: B3 fibres suffered more damage than B1 fibres. This suggests that it excessively deteriorates the fibres, ultimately reducing the thermal performance of the fibreboard. As previously discussed, the Hollander beater reduces porosity after 40 minutes of treatment. Since air has a lower thermal conductivity than solid materials, a reduction in internal air content leads to an increase in the material's overall thermal conductivity.

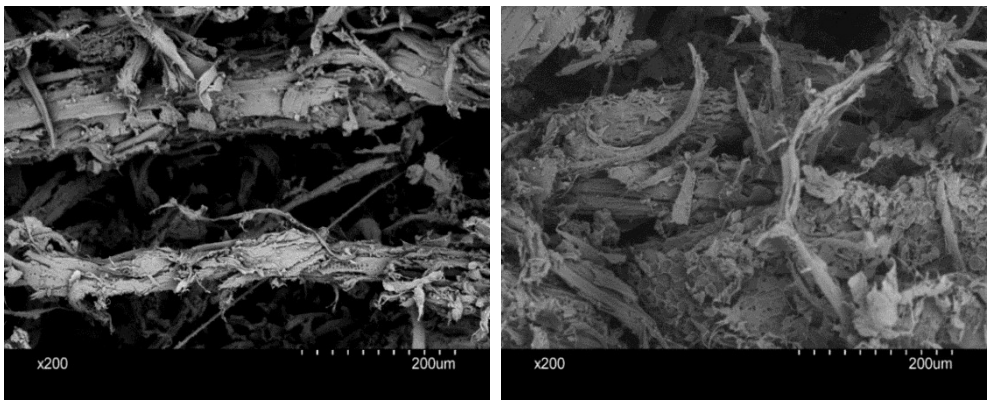

Fig. 6. SEM micrographs of B1 ×200 (left), and B3 ×200 (right).

3.6 Infrared spectrometry

Figure 7 shows the absorption spectrum detected by Fourier Transform Infrared Spectroscopy (FTIR) for different insulation samples made from bush, pine, and poplar. This spectrum allows us to examine the various bonded stretching bands present in each material and, therefore, their correlation with the different manufacturing methods.

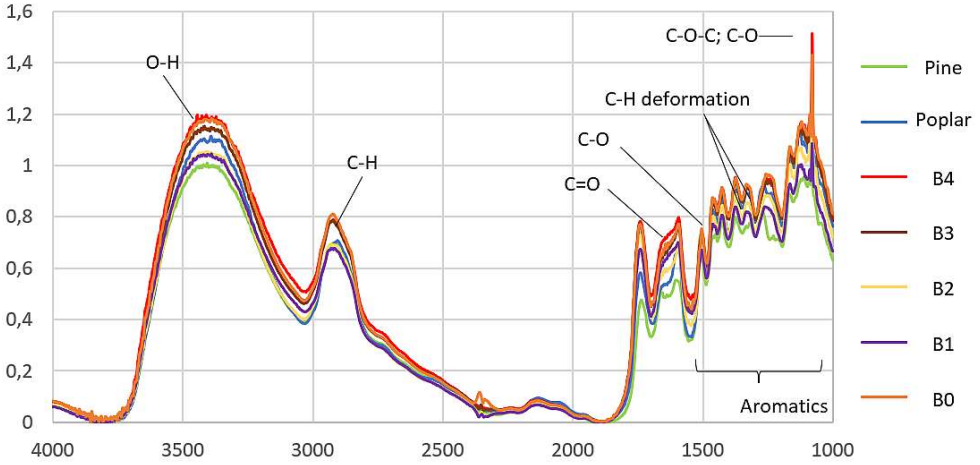

Fig. 7. FTIR absorption spectrum.

As we can see, the main reactive groups present in wood fibres are aromatic and phenolic hydroxyl groups representative of lignin. Peaks at 1600 cm^{-1} and 1500 cm^{-1} are characteristic of lignin, meaning that the higher these peaks are, the greater the lignin content [9]. As expected, lignin was not removed from the fibres. During the drying process, however, some curing may have occurred through the functional groups of lignin, contributing to stronger panel formation.

The peak at 1734 cm^{-1} indicates the presence of hemicellulose [9], allowing us to determine that the bush samples contain more hemicellulose than the pine and poplar samples.

This analysis enables us to compare the stretching intensity among different types of materials. As shown in Figure 7, B0, B4, and B3 exhibit the highest internal bonding intensity. These results can also be associated with moisture content: the higher the moisture content, the more hydrogen bonds may develop. However, it should be noted that for similar moisture levels, some inaccuracies in absorption rate measurements may occur.

3.7 Thermal conductivity

When we compare our data in Table 5 with the data in Table 6 as quoted in the literature [10], the thermal conductivity of our binderless fibreboard falls within the uncertainty range of wood fibres. According to DIN 4108 “Thermal insulation and energy economy in buildings,” materials must have a λ-value ≤ 0.1 W/(m·K) to be classified as thermal insulation materials. Our insulation material can therefore be considered as having moderate to relatively high thermal conductivity.

Table 5. Thermal conductivity coefficient (λ).

Specimens	λ-values [W/(m·K)] average ± s.d.
B0	0.0791 ± 0.0031
B1	0.0809 ± 0.0074
B2	0.0691 ± 0.0044
B3	0.0779 ± 0.0093
B4	0.0948 ± 0.0089
Pine	0.0707 ± 0.0034
Poplar	0.0682 ± 0.0055

Table 6. Insulators data from literature research.

Insulation material	Density [kg/m^3] average ± s.d.	Thermal conductivity [W/(m·K)] average ± s.d.	References
Cellulose fibres	30-80	0.04-0.045	[2]
Bagasse	70-350	0.046-0.055	
Coconut	70-125	0.04-0.05	
Wood wool	350-600	0.09	
Wood fibres	30-270	0.04-0.09	

When we compare the moisture content of each fibreboard with its respective λ-value in Figure 8, we observe a linear correlation: the higher the moisture content, the higher the thermal conductivity.

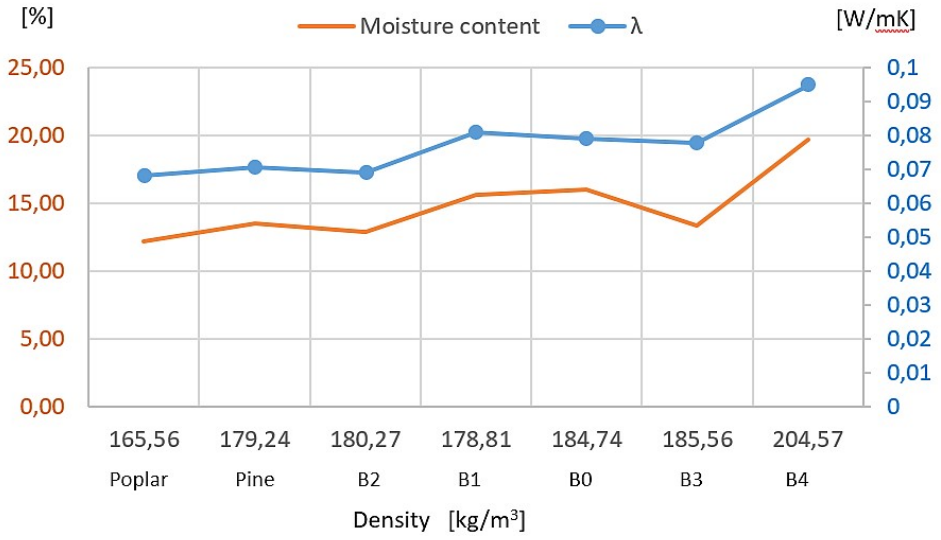

Fig. 8. λ-values and moisture contents as a function of density.

3.8 Thermogravimetry

Thermal degradation can be divided into three major stages for all samples. In the low-temperature range (up to 160°C), absorbed water evaporates. In the next two stages, the thermal decomposition of lignocellulosic materials. During the second stage, the carbohydrate fractions – namely hemicellulose and cellulose – are decomposed. This leads to a significant weight loss observed between 250°C and 420°C.

In the third stage, more heat-resistant aromatic compounds decompose. In other words, this stage corresponds to the decomposition of lignin, which occurs over a broad temperature range starting at 160°C and extending up to 800°C [11]. The extended curve starting around 430°C reflects the gradual decomposition of lignin. The weight loss in each stage is shown in Table 7.

Table 7. Weight loss of the samples.

Weight loss [%]					DTG peak T_{max} [°C]
Sample name	**Stage 1**	**Stage 2**	**Stage 3**	**Total**	
B0	10.25	56.19	10.63	77.07	380.37
B1	10.87	54.4	11.58	76.85	379.46
B2	10.15	57.44	10.31	77.90	379.33
B3	12.11	55.18	10.87	78.16	379.79
B4	12.11	55.03	10.51	77.65	380.58
Pine	7.82	62.14	10.34	80.30	383.06
Poplar	9.11	62.74	9.14	80.99	379.32

Derivative thermogravimetric (DTG) curves provide a more accurate view of thermal events (Table 7 last column). DTG diagrams indicate the rate of weight loss, including the peak temperature at which decomposition occurs most rapidly (T_{max}) [11]. The highest decomposition rate is observed in pine, followed by poplar. For bush samples, decomposition rates vary depending on the processing method. B1 and B2 show similar decomposition rates, while B0, B3, and B4 exhibit a different but consistent rate. Peak temperatures for the maximum decomposition rates are listed in Table 7.

A shoulder appears in the DTG curves between 310°C and 360°C. Hemicellulose decomposes on the lower-temperature side of this shoulder, while cellulose decomposes at higher temperatures on the right side [12]. A less pronounced shoulder suggests a lower hemicellulose content compared to a more distinct one [13].

4 Conclusion

This study investigated the production of binderless fibreboard insulation materials using forest residues, undergrowth biomass, pine, and poplar sawdust. The aim was to develop environmentally friendly panels without synthetic adhesives while maintaining appropriate thermal insulation and mechanical properties.

The experimental results demonstrated that the manufacturing method significantly influenced the material characteristics. Among the tested approaches, the fibreboard produced from undergrowth biomass with 40 minutes of Hollander beater treatment (B2) achieved the most favourable balance of density, porosity, moisture content, and thermal conductivity. In particular, B2 panels exhibited a relatively low λ-value (0.0691 W/(m·K)), a moderate density, and improved fibre morphology compared to untreated or over-treated samples.

Conversely, the pre-soaking of biomass in water for three days before defibration (B4) was found to be ineffective, leading to increased density and moisture content, which negatively impacted thermal insulation performance.

Thermogravimetric analysis confirmed that the thermal stability of the bush-based panels was comparable to those made from traditional pine and poplar sawdust. The FTIR analysis indicated that the self-bonding properties were primarily facilitated by the inherent lignin and hemicellulose content of the raw materials.

Overall, this research confirms that forest residues and undergrowth biomass can be viable raw materials for producing binderless fibreboards suitable for insulation purposes. The results support the potential for utilizing these underused resources in sustainable construction, thereby contributing to recycling economy principles and reducing reliance on synthetic binders. Future research should further optimize processing techniques to enhance the mechanical strength, durability, and long-term performance of such eco-friendly panels. According to the results of this study the potential for industrial production is really promising based on the abundantly available and low-cost raw materials and the worked-out technology with quite simple technology. That is why this material could be recommended for industrial production.

Acknowledgement

This article was prepared in the frame of the REHOUSE project (Renovation packagEs for HOlistic improvement of EU's bUildingS Efficiency, maximizing RES generation and costeffectiveness, supported by the European Commission EU Programme Horizon-CL5-2021D4-02-02 under Grant Agreement Number: 101079951. The authors would like to thank the rest of the REHOUSE partners for their support. All related information of the project is available at https://rehouse-project.eu/

References

1. F. Di Gruttola, D. Borello, Sustainability **13**(14), 7882 (2021)
2. S. Schiavoni, F. D′Alessandro, F. Bianchi, F. Asdrubali, Renew. Sustain. Energy Rev. **62**, 988-1011 (2016)
3. J.E.G. van Dam, M.J.A. van den Oever, E.R.P. Keijsers, Ind. Crops Prod. **20**(1), 97-101 (2004)
4. Z. Pásztory, I. Ronyecz Mohácsiné, Z. Börcsök, Constr. Build. Mater. **147**, 733-735 (2017)
5. L.D.H. Anh, Z. Pásztory, J. Build. Eng. **44**, 102604 (2021)
6. P. Rebolledo, A. Cloutier, M.-C. Yemele, Fibers, **6**(4), 81 (2018)
7. S.S. Shrestha, J. Tiwari, A. Rai, D.E. Hun, D. Howard, A.O. Desjarlais, M. Francoeur, T. Feng, Int. J. Therm. Sci. **187**, 108164 (2023)
8. M. Palumbo, A.M. Lacasta, N. Holcroft, A. Shea, P. Walker, Constr. Build. Mater. **124**, 269-275 (2016)
9. H. Luo, L. Yue, N. Wang, H. Zhang, X. Lu, Wood Res. **59**, 861-869 (2014)
10. M. Pfundstein, *Properties of insulating materials*, in Insulating Materials: Principles, Materials, Applications (Birkhäuser, München, 2008)
11. C. Tangsathitkulchai, S. Junpirom, J. Katesa, J. Nanomater. **2016**, 1-10 (2016)
12. C. Agarwal, Z. Kóczán, Z. Börcsök, K. Halász, Z. Pásztory, Carbohydr. Polym. **271**, 118409 (2021)

13. D. Vamvuka, E. Kakaras, E. Kastanaki, P. Grammelis, Fuel **82**(15-17), 1949-1960 (2003)
14. Canadian Wood Council, Wood Structure presentation, https://cwc.ca/